NASA Contractor Report 191110

An Asymptotic Theory of Supersonic Propeller Noise

Edmane Envia
Sverdrup Technology, Inc.
Lewis Research Center Group
Brook Park, Ohio

May 1992

Prepared for
Lewis Research Center
Under Contract NAS3–25266

National Aeronautics and Space Administration

AN ASYMPTOTIC THEORY OF SUPERSONIC PROPELLER NOISE

Edmane Envia
Sverdrup Technology, Inc.
Lewis Research Center Group
Brook Park, Ohio 44142

Abstract

A theory for predicting the noise field of supersonic propellers with realistic blade geometries is presented. The theory, which utilizes a large-blade-count approximation, provides an efficient formula for predicting the radiation of sound from all three sources of propeller noise. Comparisons with a full numerical integration indicate that the levels predicted by this formula are quite accurate. Calculations also show that, for high speed propellers, the noise radiated by the Lighthill quadrupole source is rather substantial when compared with the noise radiated by the blade thickness and loading sources. Results from a preliminary application of the theory indicate that the peak noise level generated by a supersonic propeller initially increases with increasing tip helical Mach number, but it eventually reaches a plateau and does not increase further. The predicted trend shows qualitative agreement with the experimental observations.

Introduction

Over the last dozen years, the renewed interest in supersonic propeller (propfan) technology on the one hand, and the drive to meet stringent community and cabin noise regulations on the other, have spurred a great deal of theoretical and experimental research activity in the area of high speed rotor noise.

On the theoretical side in particular significant strides have been made towards the development of accurate theories for predicting supersonic propeller noise. The foundation for almost all of these theories has been the Ffowcs Williams and Hawkings[1] (FW-H) equation, which provides a theoretical basis for calculating the radiation of sound from the propeller blade surfaces (i.e., thickness and loading noise) as well as the sound generated by the flow field surrounding the propeller disc (i.e., Lighthill quadrupole noise). The noise generated by thickness and loading sources has received a great deal of attention as exemplified by the theories of Hanson[2] and Farassat.[3] In contrast, most of the research in the area of propeller quadrupole noise has been of an exploratory nature (see, for example, Hanson and Fink[4]) even though conclusions from these efforts have suggested

that quadrupole radiation could be potentially significant for supersonic rotors. Recent work by Peake and Crighton,[5] however, has reinforced the notion that quadrupole radiation must be accounted for in predicting the noise generated by high speed propellers.

From a computational point of view, prediction of propeller noise involves evaluation of the multiple integrals appearing in FW-H equation. This task can be accomplished by various methods but, in general, an accurate and detailed prediction requires the use of numerical integration. That, in turn, necessitates the utilization of a large number of source points to produce a realistic representation of the propeller geometry as well as the flow field surrounding it. In practice, the number of thickness and loading sources necessary for such a representation is sufficiently small so as to make the computation of radiation by these two types of sources quite feasible. In contrast, a substantially larger number of quadrupole sources needed for a faithful representation of flow field around a propeller disc makes quadrupole noise computations considerably less viable. While the application of various simplification schemes like the far-field approximation has yielded some measure of success, a realistic calculation has, for the most part, remained computationally expensive.

An appealing method for circumventing this problem, first suggested by Hawkings and Lawson[6] in the context of a frequency-domain analysis, is the use of the large-blade-count approximation to calculate the source distribution integrals appearing in FW-H equation asymptotically. For modern, many-bladed propfan designs this approach offers a very effective alternative to direct numerical integration. The effectiveness of this approach was demonstrated by Crighton and Parry,[7] who developed an asymptotic theory for propeller thickness and loading noise radiation. In fact, this theory was also used by the authors in Ref. 5 to assess the importance of propeller quadrupole noise. To date, however, the published results of this theory have been limited to propellers with fairly simple geometries. Therefore, as it stands, there is a gap between the theories which utilize full numerical integration and can accommodate realistic blade geometries but are rather unwieldy for calculating noise radiation from quadrupole sources, and the asymptotic theory of Ref. 5, which is quite efficient for quadrupole noise calculations but, so far, is restricted to simple geometries.

The theory presented in this paper bridges that gap. It utilizes a large-blade-count approximation to evaluate integrals in FW-H equation. But, unlike Refs. 5 and 7, the asymptotics is applied to the radiation efficiency integrals instead of source distribution integrals. This approach affords the flexibility of using realistic blade geometries while keeping the computer time requirements small. The asymptotic analysis for thickness and loading noise sources was presented in Envia[8] and shown to provide a very good agreement with direct numerical integration. The theory is now extended to include quadrupole noise and, therefore, for the sake of completeness the full analysis will be detailed here. Comparisons with a full numerical integration will then be shown and a preliminary application of the theory to a practical problem of interest will be presented.

Analysis

The starting point for the analysis is Goldstein's[9] version of FW-H equation for the acoustic pressure $p(\mathbf{x}, t)$ written in the propeller-fixed (wind tunnel) coordinate system:

$$p(\mathbf{x},t) = -\int_{-\infty}^{+\infty}\int_{S(\tau)} \rho_0 v_n \frac{D_0 G}{D\tau}\, ds(\mathbf{y})\, d\tau + \int_{-\infty}^{+\infty}\int_{S(\tau)} f n_j \frac{\partial G}{\partial y_j}\, ds(\mathbf{y})\, d\tau$$

$$+ \int_{-\infty}^{+\infty}\int_{V(\tau)} T_{jk} \frac{\partial^2 G}{\partial y_j \partial y_k}\, d\mathbf{y}\, d\tau \qquad (1a)$$

$$T_{jk} = \rho u_j u_k + \delta_{jk}\left[(p - p_0) - C_0^2(\rho - \rho_0)\right] \qquad (1b)$$

$$\frac{D_0}{D\tau} = \frac{\partial}{\partial \tau} + U_{0_j}\frac{\partial}{\partial y_j} \qquad (1c)$$

where v_n is the normal component of the blade surface velocity, f is the amplitude of the aerodynamic loading on the blade and T_{jk} is the Lighthill stress tensor. ρ, p and u_j are the fluid density, pressure and velocity with the subscript "0" denoting their ambient values. The velocities u_j and v_n are given relative to a medium-fixed coordinate system even though Eq. (1a) is expressed in a propeller-fixed coordinate system. $S(\tau)$ and $V(\tau)$ represent the propeller blade surfaces and volume surrounding the blades, respectively, and n_j is the component of the outward unit normal to S. It should be noted that the convention for the direction of unit normal is opposite that of Goldstein's. $\mathbf{y}$ and $\mathbf{x}$ represent the source and observer coordinates, respectively. τ is the source time and t is the observer (i.e., retarded) time. U_{0_j} denotes the medium convection velocity which is equal to, and negative of, the propeller forward flight velocity. The three terms in Eq. (1a) represent contributions from the thickness, loading, and Lighthill stress (quadrupole) sources of propeller noise, respectively.

$G = G(\mathbf{x}, t/\mathbf{y}, \tau)$ in Eq. (1a) denotes the free-space, moving-medium Green's function which can be shown to have the following form:

$$G = \frac{1}{4\pi\kappa R}\,\delta(t - \tau - g_c R/C_0) \qquad (2a)$$

$$g_c(\tau) = \frac{1}{\beta_0^2}(\kappa - M_{0_R}), \qquad \kappa(\tau) = \left(M_{0_R}^2 + \beta_0^2\right)^{1/2} \qquad (2b)$$

$$M_{0_R}(\tau) = M_{0_j}\, e_j, \qquad \beta_0 = (1 - M_{0_j}^2)^{1/2} \qquad (sum\ over\ j) \qquad (2c)$$

$$M_{0_j} = \frac{U_{0_j}}{C_0}, \qquad e_j(\tau) = \frac{(x_j - y_j)}{R}, \qquad R(\tau) = |\mathbf{x} - \mathbf{y}(\tau)|. \qquad (2d)$$

Here M_{0_R} is the medium convection Mach number in the radiation direction, R is the distance between observer and source, e_j is the component of the unit vector along radiation direction, and C_0 is the medium ambient speed of sound. Parameters g_c and κ represent the effects of medium convection on the retarded time and spherical spreading rate, respectively. The explicit dependence of various parameters on source time τ is indicated where necessary.

In general, because propeller may be operating at an angle of attack to the oncoming flow, the 1-axis is chosen to coincide with the propeller shaft (see Fig. 1) in order to simplify the description of the source motion. As a result, motion of the sources is confined to the transverse planes described by the 2– and 3–axes. Therefore, it is readily seen that

$$M_{0_1} = M_0 \cos\alpha, \qquad M_{0_2} = 0, \qquad M_{0_3} = M_0 \sin\alpha \tag{3}$$

where α is the propeller angle of attack with respect to oncoming flow as depicted in Fig. (1).

Provided that blade geometry, aerodynamic loading, and flow field about the propeller are known in sufficient detail, acoustic pressure $p(\mathbf{x},t)$ may be computed directly from Eq. (1a) for any observer location. This, of course, is the so-called time domain approach which entails solving transcendental equations for source time τ. Alternatively, one could use the frequency domain approach, which involves expanding $p(\mathbf{x},t)$ in terms of its Fourier harmonic components $p_l(\mathbf{x})$, i.e.,

$$p(\mathbf{x},t) = \sum_{l=-\infty}^{+\infty} p_l(\mathbf{x})\, e^{-il\Omega t} \tag{4a}$$

with the individual harmonic components given by:

$$p_l(\mathbf{x}) = p_{T_l}(\mathbf{x}) + p_{L_l}(\mathbf{x}) + p_{Q_l}(\mathbf{x}) \tag{4b}$$

where

$$p_{T_l}(\mathbf{x}) = \frac{\Omega}{2\pi}\int_0^{2\pi/\Omega} e^{il\Omega t}\left[\int_{-\infty}^{+\infty}\int_{S(\tau)} \rho_0 v_n \frac{D_0 G}{Dt}\, ds(\mathbf{y})\, d\tau\right] dt \tag{4c}$$

$$p_{L_l}(\mathbf{x}) = -\frac{\Omega}{2\pi}\int_0^{2\pi/\Omega} e^{il\Omega t}\left[\int_{-\infty}^{+\infty}\int_{S(\tau)} f n_j \frac{\partial G}{\partial x_j}\, ds(\mathbf{y})\, d\tau\right] dt \tag{4d}$$

$$p_{Q_l}(\mathbf{x}) = \frac{\Omega}{2\pi}\int_0^{2\pi/\Omega} e^{il\Omega t}\left[\int_{-\infty}^{+\infty}\int_{V(\tau)} T_{jk} \frac{\partial^2 G}{\partial x_j \partial x_k}\, dy\, d\tau\right] dt \tag{4e}$$

in which Ω is the propeller angular speed. p_{T_l}, p_{L_l} and p_{Q_l} denote contributions to the harmonic component p_l from the thickness, loading, and quadrupole sources, respectively. In writing Eqs. (4c-4e) the derivatives of G with respect to source coordinates from Eq. (1a) have been replaced by its derivatives with respect to observer coordinates through use of the relations

$$\frac{\partial G}{\partial y_j} = -\frac{\partial G}{\partial x_j}, \qquad \frac{D_0 G}{D\tau} = -\frac{D_0 G}{Dt}. \tag{5}$$

Using the usual phase relationship arguments it can be shown that, given B identical blades, only harmonic components for which $l = mB$ (where m is an integer) contribute

to the infinite sum in Eq. (4a). This contribution is simply B times the contribution of a single blade. Therefore, from here on B will explicitly appear in expressions for the harmonic components $p_{\mathcal{T}_{mB}}$, $p_{\mathcal{L}_{mB}}$, and $p_{\mathcal{Q}_{mB}}$. Correspondingly, S and V, respectively, will denote surface of, and volume around, a single blade.

To further simplify Eqs. (4c-4e) the spatial derivatives $\partial/\partial x_j$ and $\partial^2/\partial x_j \partial x_k$ of G may be rewritten in terms of the temporal derivative $\partial/\partial t$ through the use of the chain rule:

$$\frac{\partial G}{\partial x_j} = \mathcal{D}_j(t) G \tag{6a}$$

$$\frac{\partial^2 G}{\partial x_j \partial x_k} = \left[\frac{\partial \mathcal{D}_k(t)}{\partial x_j} + \mathcal{D}_j(t)\mathcal{D}_k(t) \right] G \tag{6b}$$

$$\mathcal{D}_j(t) = -\left[\frac{1}{C_0 \kappa} \left(e_j - g_c M_{0_j} \right) \frac{\partial}{\partial t} + \frac{1}{\kappa^2 R} \left(\beta_0^2 e_j + M_{0_R} M_{0_j} \right) \right] \tag{6c}$$

where the auxiliary derivative operator $\mathcal{D}_j(t)$ has been introduced for notational brevity. The temporal derivatives can now be removed using integration by parts, and the integral over t, which involves a delta function, can then be easily evaluated to yield

$$p_{\mathcal{T}_{mB}}(\mathbf{x}) = \frac{B\Omega}{8\pi^2} \int_0^{2\pi/\Omega} \left[\int_{S(\tau)} \left(\sum_{\ell=1}^{2} \frac{Q_{\mathcal{T}}^{(\ell)}}{R^\ell} \right) e^{imB\Omega(\tau + g_c R/C_0)} \, ds(\mathbf{y}) \right] d\tau \tag{7a}$$

$$p_{\mathcal{L}_{mB}}(\mathbf{x}) = \frac{B\Omega}{8\pi^2} \int_0^{2\pi/\Omega} \left[\int_{S(\tau)} \left(\sum_{\ell=1}^{2} \frac{Q_{\mathcal{L}}^{(\ell)}}{R^\ell} \right) e^{imB\Omega(\tau + g_c R/C_0)} \, ds(\mathbf{y}) \right] d\tau \tag{7b}$$

$$p_{\mathcal{Q}_{mB}}(\mathbf{x}) = \frac{B\Omega}{8\pi^2} \int_0^{2\pi/\Omega} \left[\int_{V(\tau)} \left(\sum_{\ell=1}^{3} \frac{Q_{\mathcal{Q}}^{(\ell)}}{R^\ell} \right) e^{imB\Omega(\tau + g_c R/C_0)} \, dy \right] d\tau \tag{7c}$$

where $Q_{\mathcal{T}}^{(\ell)}$, $Q_{\mathcal{L}}^{(\ell)}$ and $Q_{\mathcal{Q}}^{(\ell)}$ represent the expressions for the strengths of thickness, loading and quadrupole sources, respectively. Note that the $Q_{\ldots}^{(\ell)}$s for each source type are organized according to which power of radiation distance R they multiply. Note also that the limits on the integration over τ have been changed to reflect the fact that an interval of size $2\pi/\Omega$ in t is mapped exactly into an interval of size $2\pi/\Omega$ in τ. The expressions for source strengths are given by

$$Q_{\mathcal{T}}^{(1)} = -\frac{1}{\kappa^2} \, imB\Omega \, \rho_0 v_n \left[1 - \frac{1}{\kappa} M_{0_j} (e_j - g_c M_{0_j}) \right] \tag{8a}$$

$$Q_{\mathcal{T}}^{(2)} = -\frac{1}{\kappa^3} \, \rho_0 v_n \, M_{0_j} \left(\beta_0^2 e_j + M_{0_R} M_{0_j} \right) \tag{8b}$$

$$Q_{\mathcal{L}}^{(1)} = -\frac{1}{C_0\kappa^2}\, imB\Omega\, fn_j\left(e_j - g_c M_{0_j}\right) \tag{8c}$$

$$Q_{\mathcal{L}}^{(2)} = \frac{1}{\kappa^3}\, fn_j\left(\beta_0^2 e_j + M_{0_R} M_{0_j}\right) \tag{8d}$$

$$Q_{\mathcal{Q}}^{(\ell)} = \frac{1}{\kappa^{\ell+2}}\, T_{jk}\Big[\mathcal{A}_1^{(\ell)}\delta_{jk} + \mathcal{A}_2^{(\ell)} e_j e_k + \mathcal{A}_3^{(\ell)} M_{0_j} M_{0_k} + \mathcal{A}_4^{(\ell)}\left(e_j M_{0_k} + M_{0_j} e_k\right)\Big] \qquad \ell = 1,2,3 \tag{8e}$$

$$\begin{aligned}
&\mathcal{A}_1^{(1)} = 0, && \mathcal{A}_2^{(1)} = 1, && \mathcal{A}_3^{(1)} = g_c^2, && \mathcal{A}_4^{(1)} = -g_c,\\
&\mathcal{A}_1^{(2)} = -\kappa^2, && \mathcal{A}_2^{(2)} = 3\beta_0^2, && \mathcal{A}_3^{(2)} = -(1 + 2M_{0_R} g_c), && \mathcal{A}_4^{(2)} = 2M_{0_R} - \beta_0^2 g_c,\\
&\mathcal{A}_1^{(3)} = -\beta_0^2\kappa^2, && \mathcal{A}_2^{(3)} = 3(\beta_0^2\kappa^2 - M_{0_R}^2), && \mathcal{A}_3^{(3)} = (3M_{0_R}^2 - \kappa^2), && \mathcal{A}_4^{(3)} = 3\beta_0^2 M_{0_R}.
\end{aligned} \tag{8f}$$

where sums over the indices j and k are assumed. It should be noted that, in general, normal surface velocity v_n, loading amplitude f, and the Lighthill stress tensor T_{ij} depend on source time τ.

Once source strength distributions $Q_{\cdots}^{(\ell)}$ are estimated, what remains is to carry out the integrations in Eqs. (7a-7c). Ordinarily, the order of integration in these equations is reversed and the integral over τ (which represents the radiation efficiency of the acoustic source) is computed first. Since for general geometries and source strengths this integral is not tractable analytically, it is usually computed approximately for near- or far-field observer locations for which the integrand may be significantly simplified. The result is given in terms of the appropriate Bessel functions. The remaining surface (or volume) integral is then carried out using a quadrature scheme. Alternatively, as was mentioned earlier, surface (or volume) integral may be calculated asymptotically in the manner suggested in Ref. 6. In this approach, which is particularly useful when the blade count B (or more appropriately the harmonic index mB) is large, the method of stationary phase is utilized to show that, asymptotically, most of the radiation from blade surface (or volume surrounding it) comes from the neighborhood of special points called the stationary phase points. As was pointed out in introduction, this approach forms the basis of theory presented in Refs. 5 and 7. The utility of this approach hinges on determining, analytically, the stationary phase points – a difficult task when dealing with blades having complicated geometries.

This difficulty, however, can be circumvented by applying the large-blade-count approximation to integral over τ instead. In other words, the idea is to find the radiation efficiency of each source asymptotically. This is accomplished by evaluating the τ integral using a modification to the standard steepest descent and saddle point methods. The advantage of this approach is that it is applicable to general geometries.

In this paper the derivation for the zero angle of attack case ($\alpha = 0$) will be outlined. The extension to nonzero angle of attack follows the analysis described in Ref. 8. For the sake of brevity the final formula will be given in terms of a generic source strength Q and

a generic radiation distance "factor" $\mathcal{R}$. The resulting expression is therefore applicable to any $Q^{(\ell)}_{\cdots}$ and R^{ℓ} dependence.

For practical considerations it is more convenient to preserve the order of integration in Eqs (7a-7c) and carry out surface (or the volume) integral first. To do so, we begin by dividing blade surface (or volume surrounding it) into a number of small surface (or volume) elements. Let that number be N_s, where the subscript s indicates a particular source element under consideration. If the typical elemental size is sufficiently small, integrand may be assumed to be constant over the extent of element and thus surface (or volume) integral may be approximated by some appropriate "mean value" of integrand times the elemental surface area (or volume). If the mean value is chosen to be the value of integrand at the geometric center of element, designated $\mathbf{y_s}$, the error in this approximation is $O(L^2)$ for a given N_s where $L = |\mathbf{y} - \mathbf{y_s}|_{\max}$. Of course, error could be made arbitrarily small by choosing a large enough N_s, which would reduce the effective size of each element.

Therefore, the generic harmonic amplitude $\mathcal{P}_{s_{mB}}(\mathbf{x})$ may be written as:

$$\mathcal{P}_{s_{mB}}(\mathbf{x}) \simeq \frac{1}{\Omega} \sum_{s=1}^{N_s} \Delta_s \, e^{-imB\Psi_{C_s}} \, I_s \tag{9a}$$

$$I_s = \int_0^{2\pi} \frac{Q_s(\theta)}{\mathcal{R}_s(\theta)} \, e^{mB\Phi_s(\theta)} \, d\theta \tag{9b}$$

$$\Phi_s(\theta) = i\left(\theta + a_s\sqrt{1 - b_s\cos\theta}\right) \tag{9c}$$

$$\theta = \Omega\tau + \phi_s - \phi, \qquad \Psi_{C_s} = \frac{M_{tip}M_{0_1}}{\beta_{0_1}^2}(x_1 - y_{1_s}) + \phi_s - \phi \tag{9d}$$

$$a_s = \frac{M_{tip}}{\beta_{0_1}\sqrt{\mathcal{X}_s^2 + r^2 + r_s^2}}, \qquad b_s = \frac{2rr_s}{\mathcal{X}_s^2 + r^2 + r_s^2} \tag{9e}$$

$$\mathcal{X}_s = \frac{1}{\beta_{0_1}}(x_1 - y_{1_s}), \qquad \beta_{0_1} = (1 - M_{0_1}^2)^{1/2} \tag{9f}$$

where (x_1, x_2, x_3) and $(y_{1_s}, y_{2_s}, y_{3_s})$ have been replaced by their cylindrical polar counterparts (x_1, r, ϕ) and (y_{1_s}, r_s, ϕ_s), respectively. Furthermore, the integration variable τ is now replaced by a new variable θ. M_{tip} is the tip rotational Mach number (i.e., $R_{tip}\Omega/C_0$) and Ψ_{C_s} is a convective phase factor representing the collection of phase terms which do not depend on τ. $Q_s(\theta)$ and $\mathcal{R}_s(\theta)$ are the generic source strength and radiation distance factor, and Δ_s is elemental area (or volume) for the sth element. In order to simplify the notation, we suppress the explicit dependence of various variables on $\mathbf{y_s}$, the centroid of sth element. $\Phi_s(\theta)$ is the canonical phase function for a propeller operating at zero angle of attack, with a_s and b_s representing a combination of geometric, convective and kinematic factors. Note that in deriving $\Phi_s(\theta)$, no assumption regarding the geometry of propeller blade or the location of observer has been made. For this reason, the subsequent results apply to arbitrary geometries and observer locations. In the above expressions both observer and source spatial coordinates are nondimensionalized by the propeller tip radius R_{tip}. (Note that $M_{0_1} = M_0$ for zero angle of attack case.)

Now, for a typical propfan $B = 8$. Thus even for the blade-passing-frequency (BPF) tone (i.e., $m = 1$) the integrand in Eq. (9b) is highly oscillatory. Nallasamy et al.,[10] who considered only the thickness and loading noise contributions, employed a numerical integration scheme to calculate I_s. Unfortunately, accurate computation of higher harmonics requires an ever increasing quadrature resolution to capture the oscillatory nature of the integrand and that can increase the computational cost substantially. The asymptotic evaluation of I_s for large mB, however, can be quite cost-effective.

In order to carry out the asymptotic evaluation, variable θ must be allowed to be complex and the integration path (i.e., $[0, 2\pi]$) be deformed into an appropriate contour. Replacing θ with the complex variable $\nu = \theta + i\sigma$ leads to a phase function $\Phi_s(\nu)$ which is now also complex. It is fairly straightforward to find the saddle points of $\Phi_s(\nu)$ (i.e., $\Phi_s'(\nu) = 0$) and the appropriate steepest descent contours. The easiest way to find the saddle points is to define an auxiliary variable $\xi = \cos\nu$ and rewrite $\Phi_s'(\nu) = 0$ in terms of ξ:

$$(a_s b_s/2)^2\, \xi^2 \; - b_s \xi + 1 - (a_s b_s/2)^2 = 0 \tag{10}$$

where a_s and b_s were defined in Eq. (9d). Eq. (10) is clearly quadratic in ξ and may readily be solved. Thus for given observer and source locations $\Phi(\nu)$ has, in general, two simple saddle points in the interval $[0, 2\pi]$ which have different forms depending on whether the component of the source relative Mach number in the direction of observer, M_r, is subsonic or supersonic. The two are a complex conjugate pair if $M_r < 1$ and are real if $M_r > 1$. When $M_r = 1$ (i.e., the "sonic condition") these two saddle points merge to give rise to a single, second order saddle point. For a subsonic source, only one of the two saddle points lies on the appropriate steepest descent path. Hence only that saddle point contributes to the integral. It should be noted that the integrand also has an infinite number of branch points coinciding with those of $\Phi_s(\nu)$, of which only four lie in the region of interest. A judicious choice of branch cuts guarantees that the contributions to the contour integral along branch cuts in the ν-plane is exponentially small compared with the contributions from the neighborhood of saddle points. The location of the appropriate saddle points, branch cuts, and steepest descent contours for typical source locations are shown in Fig. 2. Note that the choice of steepest descent path depends on whether M_r is less than or greater than unity. Also shown in this figure are the auxiliary descent contours needed for deforming the original contour $[0, 2\pi]$ into steepest descent contour(s). Due to the periodicity of integrand in θ, the contributions from these contours cancel each other out exactly.

For a given observer location and operating condition, the asymptotic structure of I_{n_p} for a source with $M_r = 1$ is different from that for a source with $M_r \neq 1$. In fact it, is fairly easy to show that the asymptotic expansion is given in terms of the inverse 1/3-powers of parameter mB for a "sonic" source and in terms of the inverse 1/2-powers of mB for a "non-sonic" one. Since there is no simple way of constructing a composite expansion from these two expansions to allow for a smooth transition through the sonic condition, they are not very convenient to use. However, this difficulty may be avoided altogether by developing a uniform asymptotic expansion using a theorem derived by Chester et al.[11] The details of the methodology may be found in Bleistein and Handelsman.[12] The basic idea is to

map, conformally (say, $\nu \rightarrow \zeta$), phase function $\Phi_s(\nu)$ into a much simpler function (i.e., a cubic polynomial) which exhibits the relevant features of the original phase function. The region of interest in complex ν-plane (i.e., the region containing saddle points and steepest descent contours) is correspondingly mapped into a region in the complex ζ-plane. The standard steepest descent and saddle point methods are then applied to the integral in the ζ-plane. The key definitions and parameters, along with the final result, are summarized below.

The cubic is given by:

$$\Phi_s(\nu) = -\left(\frac{\zeta^3}{3} - \gamma_s^2\zeta\right) + \mu_s \tag{11a}$$

$$\mu_s = \frac{1}{2}\left[\Phi_s(\nu_s^+) + \Phi_s(\nu_s^-)\right] \tag{11b}$$

$$\gamma_s^3 = \frac{3}{4}\left[\Phi_s(\nu_s^+) - \Phi_s(\nu_s^-)\right] \tag{11c}$$

where ν_s^+ and ν_s^- denote the locations of saddle points of Φ_s in complex ν-plane and μ_s and γ_s are parameters defining the conformal map. Note that γ_s as given above can take on three possible values or branches. The theorem in Ref. 11 guarantees that one of the branches defines the desired conformal map. For integral I_s the branch chosen is the one for which γ_s^2 is purely real. With these parameters determined, the map can be constructed and the uniform asymptotic expansion carried out. In principle, expansion of integral I_s could be developed to an arbitrary order in the parameter mB. However, it turns out that for most applications the first term provides a very reasonable approximation even at BPF tone (i.e., $m = 1$). Therefore, in the subsequent analysis only the first term is considered.

After a fair amount of algebra the final result can be written as the following formula:

$$I_s \simeq 2\pi i e^{mB\mu_s}\left\{d_{s_0}\frac{A_i\left((mB)^{2/3}\gamma_s^2\right)}{(mB)^{1/3}} + d_{s_1}\frac{A_i'\left((mB)^{2/3}\gamma_s^2\right)}{(mB)^{2/3}}\right\} \tag{12a}$$

$$d_{s_0} = \frac{\Gamma_0(\gamma_s) + \Gamma_0(-\gamma_s)}{2}, \qquad d_{s_1} = \frac{\Gamma_0(\gamma_s) - \Gamma_0(-\gamma_s)}{2\gamma_s} \tag{12b}$$

$$\Gamma_0(\zeta) = \frac{Q_s(\nu(\zeta))}{\mathcal{R}_s(\nu(\zeta))}\frac{d\nu}{d\zeta}, \qquad \frac{d\nu}{d\zeta} = \frac{\gamma_s^2 - \zeta^2}{\Phi_s'(\nu(\zeta))} \tag{12c}$$

where A_i and A_i' are the Airy function and its derivative, respectively, and d_{s_0} and d_{s_1} are coefficients in the asymptotic expansion. It is worth mentioning that $\pm\gamma_s$ corresponds to the locations of saddle points $\nu_s^\pm$ in ζ-plane. For any observer location, Airy function and its derivative provide a smooth transition from the region of blade for which M_r is less than unity to the region of blade for which M_r is greater than unity. For $\gamma_s = 0$ (i.e., a "sonic" source) A_i and A_i' are $O(1)$ and consequently I_s is proportional to inverse 1/3-powers of mB. For $\gamma_s \neq 0$ (i.e., a "non-sonic" source) and large mB A_i is $O((mB)^{-1/6})$ and A_i' is $O((mB)^{1/6})$. Consequently, I_s is proportional to inverse 1/2-power of mB as expected. After substituting for I_s in Eq. (9a) from Eq. (12a) and adding the contributions from all the N_s elements, Fourier harmonic component $\mathcal{P}_{mB}(\mathbf{x})$ can be calculated.

Results and Discussion

In order to assess the accuracy of the asymptotic formula given by Eq. (12a), we next consider its predictions for a test problem. The test case is that of a propfan operating at cruise conditions. The necessary aerodynamic input to the acoustic model is computed using an Euler CFD code developed by Adamczyk (see Celestina et al[13]) which provides both the loading distribution on propfan blades and flow field around the propfan. The CFD computations are for the flow conditions which roughly correspond to the wind tunnel conditions in a series of acoustic measurements carried out at NASA Lewis Research Center by Dittmar and Stang[14] for a scale model SR-7A propfan operating at simulated cruise conditions. All of the acoustic calculations presented in this paper are for BPF tone noise.

As was previously mentioned, the asymptotic formula is applicable to all three types of sources represented in Eqs. (7a-7c). The application of formula to thickness and loading noise sources (i.e., surface sources) is quite straightforward since the spatial extent of their distribution is clearly defined. However, the "effective" spatial extent of the distribution of quadrupoles (i.e., volume sources) is not known *a priori*. To determine this effective spatial extent a series of calculations employing the asymptotic formula for the quadrupole sound pressure level (SPL) was carried out using a series of progressively larger computational volumes surrounding the propfan blade.

The results of this study are shown in Fig. 3 where the predicted sideline directivities of quadrupole SPL (at BPF) for different computational volumes are plotted for near-field observer positions located at a distance of $1.6R_{tip}$ from the axis of propfan, and extending from $1.0R_{tip}$ forward to $1.0R_{tip}$ aft of the plane of rotation. The medium convection (free stream) Mach number M_0 is 0.8 and the advance ratio of propfan is 3.06, which together result in a (relative) tip helical Mach number ($M_{tip_h} = (M_0^2 + M_{tip}^2)^{1/2}$) of 1.15. As a matter of convenience the computational volumes were chosen to coincide with the subsets of the CFD computational grid. In all, four volumes were considered. The passage volume, denoted $V0$, extends axially from the blade's leading edge to its trailing edge and extends radially from hub to tip. Volume $V1$ extends axially to about $0.6R_{tip}$, volume $V2$ to $2.0R_{tip}$, and volume $V3$ to $4.0R_{tip}$ in both the forward and aft directions. The latter three volumes also extend a distance of $0.5R_{tip}$ beyond the blade tip in the radial direction. All four volumes also span the blade passage halfway to the adjacent blades in the circumferential direction on each side. For each volume the contributions to noise field from Lighthill quadrupole sources contained within the volume were computed and plotted.

Two important conclusions drawn from the plot in Fig. 3 are that (i) the predicted peak quadrupole SPL occurs in the vicinity of plane of rotation and (ii) that as far as the peak noise levels are concerned, volume $V1$ is optimally suited for acoustic calculations since the larger volumes produce levels which are generally no more than 1 dB different from those for volume $V1$ (the results for volumes $V2$ and $V3$ are virtually indistinguishable). The erratic behavior of predicted SPL for the baseline volume $V1$ at the axial observer locations aft of the $0.6R_{tip}$ position is a result of the choice of computational volume. Because, these observer locations lie near the boundary between $V1$ and $V2$, in the baseline case they only receive contributions from sources located upstream of that boundary (i.e., those inside $V1$ only). Clearly, as computational volume is extended and contributions from sources downstream of that boundary (i.e., those inside $V2$ but not inside $V1$) are

also taken into account, more realistic levels are produced and the "kink" in the SPL disappears. Furthermore, in order to verify that the kink is not an artifact of asymptotic calculations, a full numerical integration of radiation efficiency integral for volume $V1$ was performed at a few discrete locations and the results plotted as solid symbols in Fig 3. The comparison between asymptotic and numerical calculations is strikingly good and serves to demonstrate the accuracy of asymptotic calculations.

To further emphasize this accuracy, a comparison between the asymptotically and numerically computed sideline directivity of total SPL (thickness + loading + quadrupole) is presented in Fig. 4. The operating conditions and observer locations are the same as those in Fig. 3. The quadrupole contribution from volume $V1$ was considered in this comparison. The numerical integration was carried out for only five observer locations to limit the computational time. Again, the agreement is very good with deviations of less than 1 dB in plane of rotation between asymptotic and numerical results. For comparison, the corresponding sideline directivity for the noise generated by surface sources is also shown. The agreement is quite good with a maximum deviation of about 2 dB occurring at about $0.5R_{tip}$ downstream of plane of rotation. A detailed examination of the individual source type contributions in this region revealed that on the one hand the discrepancy is partly due to deviations (of around 2 dB) between the asymptotically and numerically calculated loading noise predictions, and on the other to the strong sensitivity of the sum of thickness and loading noise SPLs to their individual contributions. It is also interesting to note that the noticeably higher total SPLs as compared with those for surface sources indicate that quadrupole noise levels are rather substantial for high speed propellers and must be taken into account.

Finally, to demonstrate the utility of the method, a series of acoustic calculations was performed to investigate the sensitivity of the maximum total SPL generated by propfan as a function of its tip helical Mach number M_{tip_h}. The increase in M_{tip_h} was achieved by holding the advance ratio constant (at 3.06) and increasing the free stream Mach number M_0. The range of tip helical Mach numbers studied was between 0.9 and 1.4 with 11 different Mach numbers considered within this range. The aerodynamic input in each case was computed using the Euler code mentioned earlier. As before, the computational volume chosen for acoustic calculations was $V1$. Twelve observer positions distributed on both sides of plane of rotation were considered. These positions correspond to the microphone locations in Ref. 14. In each case the asymptotically-predicted maximum SPL was noted amongst observer positions considered. In all cases this maximum occurred in the neighborhood of plane of rotation.

The peak SPLs are plotted versus M_{tip_h} in Fig. 5. To see the trend, a quadratic curve is fitted to the predicted values (solid circles). The predicted trend indicates that maximum SPL does not increase monotonically with increasing tip helical Mach number, but rather that it levels off beyond M_{tip_h} of about 1.25. This behavior is consistent with the trends observed in the measurements reported in Ref. 14. As seen from the inset in Fig. 5, measured peak SPLs generally reach a plateau past a tip helical Mach number of about 1.25. Different symbols in the inset represent peak SPLs corresponding to different propfan blade setting angles while the lines are quadratic curve fits through the points. The advance ratio in all three cases is 3.06. In this paper no attempt was made to carry

out a detailed comparison with the experimental data due to the ambiguities which exist in matching the experimental operating conditions with their CFD counterparts. For the sake of comparison, however, the maximum SPLs as predicted from only the surface sources are also plotted (open circles) in Fig. 5. It is interesting to note that, in contrast with total noise, predicted peak noise arising from surface sources, tends to rise monotonically with the increasing tip helical Mach number. An examination of theoretical predictions shows that, the difference in behavior between peak SPLs from surface and total sources may be traced to the mutual phase relationship between surface and volume sources. For $M_{tip_h} < 1.25$, surface and volume sources radiate essentially in phase. Therefore, they contribute additively to total SPL. For $M_{tip_h} > 1.25$, however, surface and volume sources radiate out of phase. This leads to mutual cancellation between the two types of sources and, as a result, in reduced peak SPLs.

It is worth mentioning that the CPU times required for these asymptotic noise calculations were generally an order of magnitude smaller than those for full numerical integration. The CPU time savings would be even more significant for higher harmonics of BPF where numerical integration requires a progressively finer quadrature step size. In contrast, asymptotic calculations would incur a nominal increase in CPU time over that required for the BPF tone calculations, since saddle point locations are independent of the mode number. Furthermore, due to the very nature of the asymptotic expansion, predictions for the higher harmonic will be even more accurate when compared with numerical results (see Ref. 8).

Concluding Remarks

A large-blade-count asymptotic theory which allows for accurate and efficient calculation of noise field of high speed propellers was presented. The theory does not rely on the simplifying assumptions usually employed in other propeller noise analyses. A closed form expression involving Airy function and its derivative gives a uniform representation of the noise field of a source regardless of whether its component of the relative Mach number in the direction of the observer is less or greater than unity. The levels of all three types of propeller noise sources (i.e., thickness, loading, and Lighthill quadrupoles) were computed for a realistic propeller geometry and operating condition at a very reasonable computational cost. The results indicate that near-field quadrupole radiation is rather substantial in vicinity of plane of rotation and can significantly influence total sound pressure levels radiated by a supersonic propeller. Furthermore, inclusion of quadrupole contribution in predicted levels seems to generate trends which are in qualitative agreement with experimental measurements of sensitivity of maximum SPL to increases in tip helical Mach number. The preliminary results shown here indicate that the present method provides a useful theoretical tool in propeller noise research.

Acknowledgements

This work was supported under NASA grant NAS3-25266 and carried out at NASA Lewis Research Center in Cleveland, Ohio. The author wishes to thank Dr. Osamu Yamamoto and Mr. John Papp for providing him with the computed flow fields.

References

1. Ffowcs Williams, J.E. and Hawkings, D.L., "Sound Generation by Turbulence and Surfaces in Arbitrary Motion," Phil. Trans. R. Soc. Lond. Series A, Vol. 264, May 8, 1969, 321-342.
2. Hanson, D.B., "Near Field Frequency Domain Theory for Propeller Noise,"AIAA J., Vol. 23, April 1985, 499-504.
3. Farassat, F., "Linear Acoustic Formulae for Calculation of Rotating Blade Noise," AIAA J., Vol. 19, 1981 1122-1130.
4. Hanson, D.B. and M.R. Fink, "The Importance of Quadrupole Sources in Prediction of Transonic Tip Speed Propeller Noise," J. Sound Vib. 62(1), 1979, 19-38.
5. Peake N. and D.G. Crighton, "Lighthill Quadrupole Radiation in Supersonic Propeller Acoustics," J. Fluid Mech. Vol. 223, 1991, 363-382.
6. Hawkings, D.L. and Lowson, M.V., "Theory of Open Supersonic Rotor Noise," J. Sound Vib. 36(1), 1974, 1-20.
7. Crighton, D.G. and A.B. Parry, "Asymptotic Theory of Propeller Noise Part II: Supersonic Single-Rotation Propeller," AIAA J. Vol. 29, No. 12, December 1991, 2031-2037.
8. Envia E., "Prediction of Noise Field of a Propfan at Angle of Attack," Submitted to the Sixth IUTAM meeting, Notre Dame, Indiana, September 15-19, 1991, also NASA-CR 189047, October 1991.
9. Goldstein, M.E., AEROACOUSTICS, McGraw-Hill, New York, 1976, 189-192.
10. Nallasamy, M., E. Envia, B.J. Clark, and J.F. Groeneweg, "Near-Field Noise of a Single Rotation Propfan at an Angle of Attack," AIAA paper 90-3953, also NASA-TM-103645, 1990.
11. Chester, C., B. Friedman and F. Ursell, "An Extension of the Method of Steepest Descent," Proc. Camb. Phil. Soc. 53, 1957, 599-611.
12. Bleistein, N. and R.A. Handelsman, ASYMPTOTIC EXPANSIONS OF INTEGRALS, Dover Publications Inc., New York, 1986, 369-374.
13. Celestina, M.L., R.A. Mulac and J.J. Adamczyk, "A Numerical Simulation of the Inviscid Flow Through a Counterrotating Propeller," J. Turbomachinery, Vol. 108, October 1986.
14. Dittmar J.H. and D.B. Stang, "Cruise Noise of the 2/9 Scale Model of the Large-Scale Advanced Propfan (LAP) Propeller, SR7A," NASA-TM 100175.

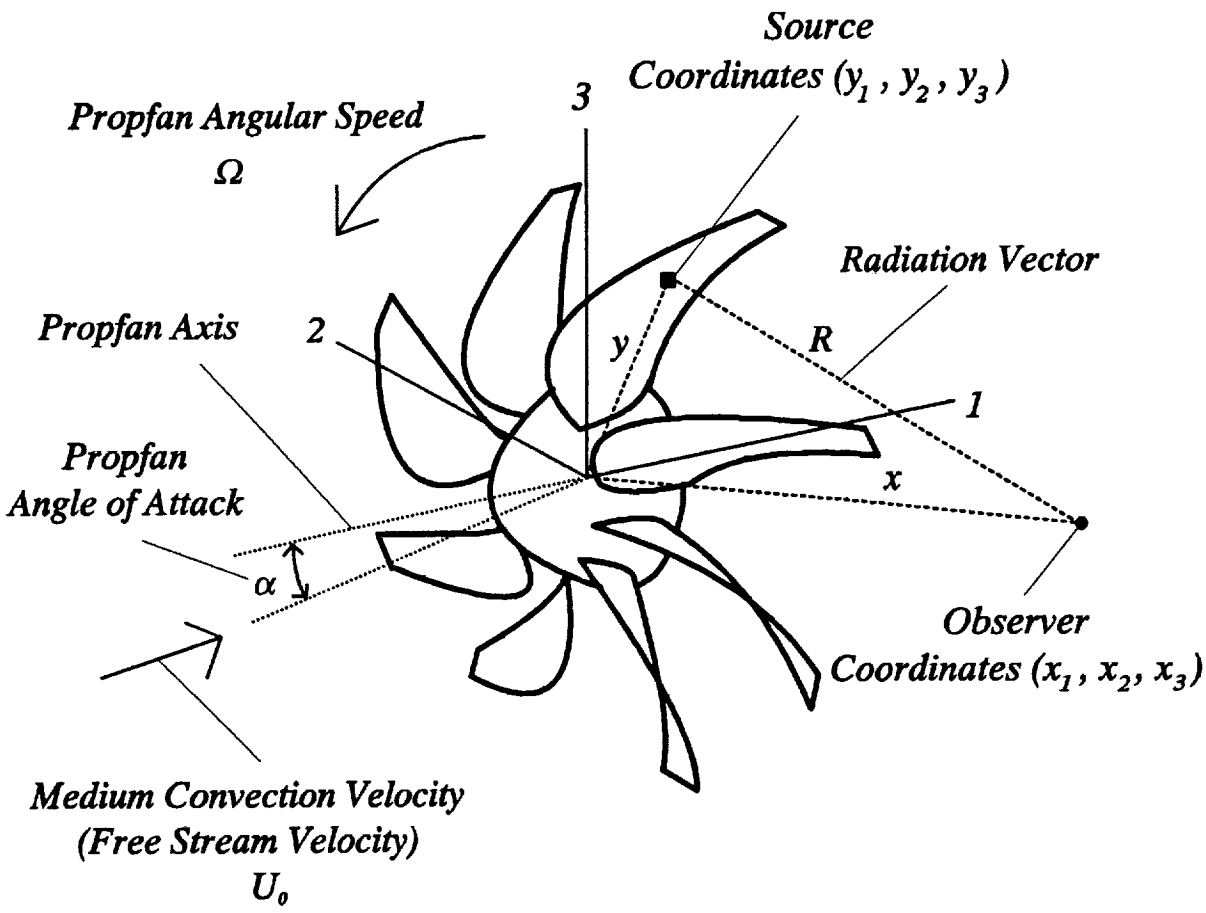

Fig. (1) Definitions of Geometry and Coordinate System.

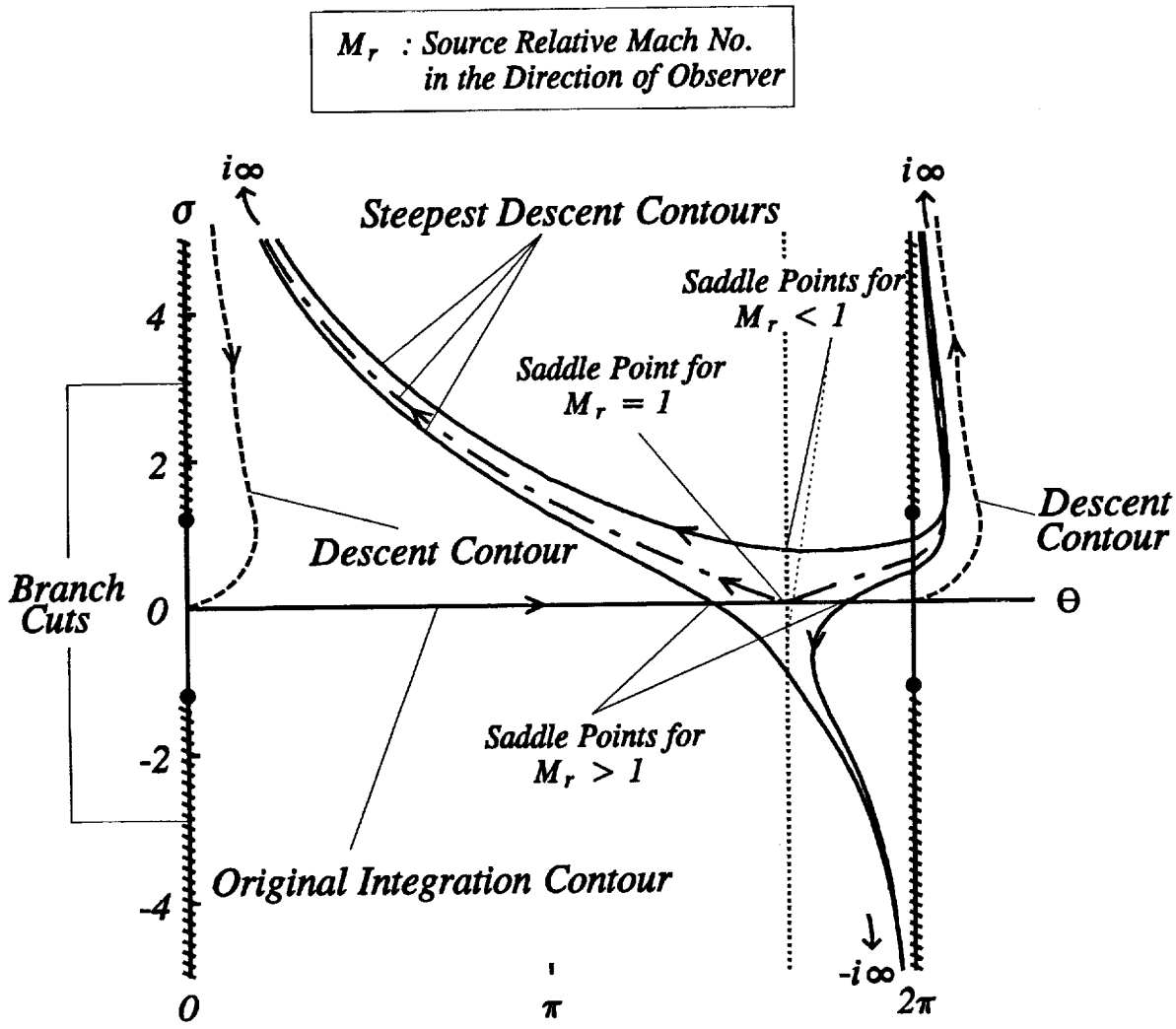

Fig. (2) Saddle Points and Steepest Descent Contours in the Complex ν-Plane.

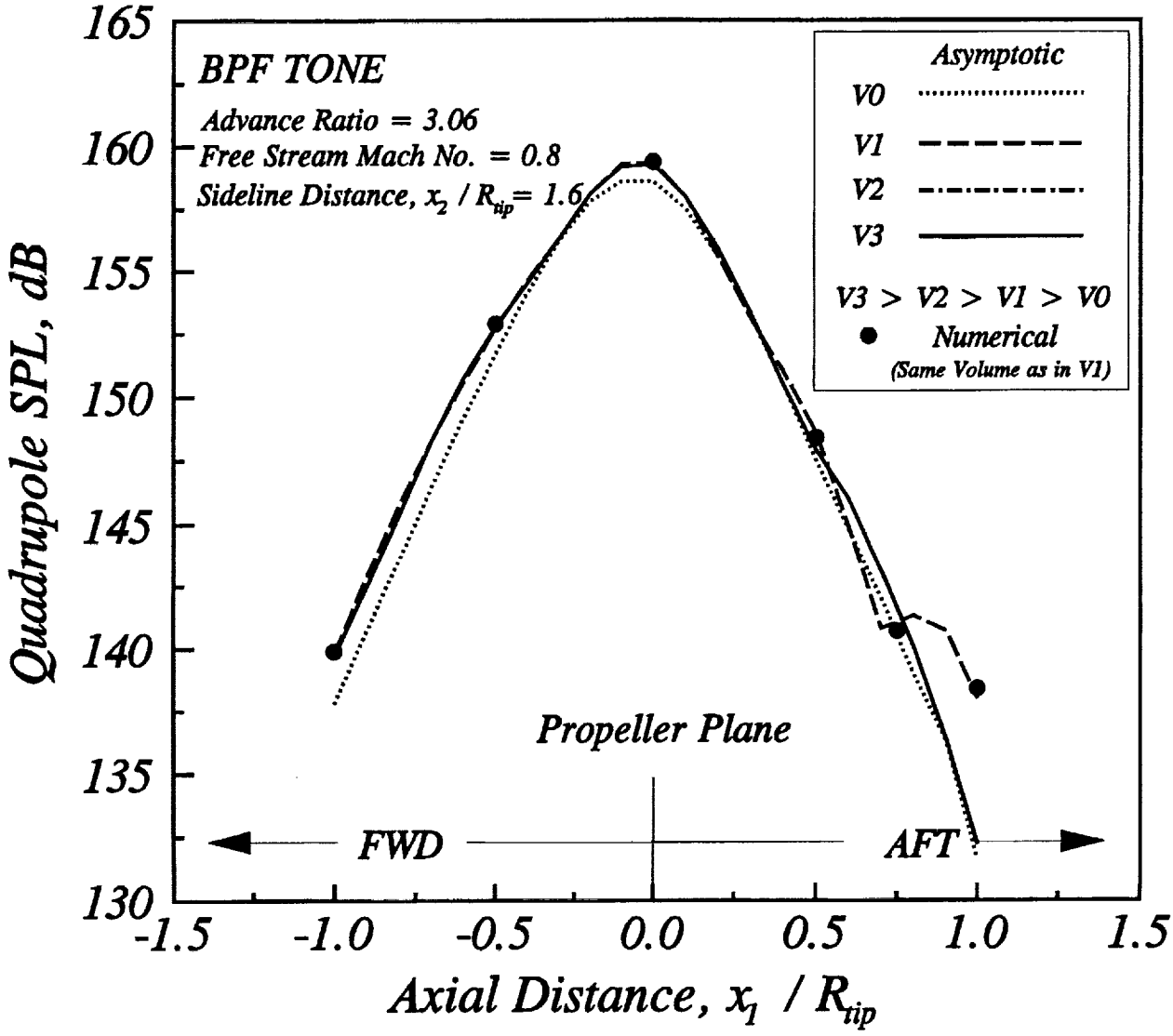

Fig. (3) Sideline Directivity of the Predicted Quadrupole SPL as a Function of the Computational Volume Chosen. (Asymptotic Calculations)

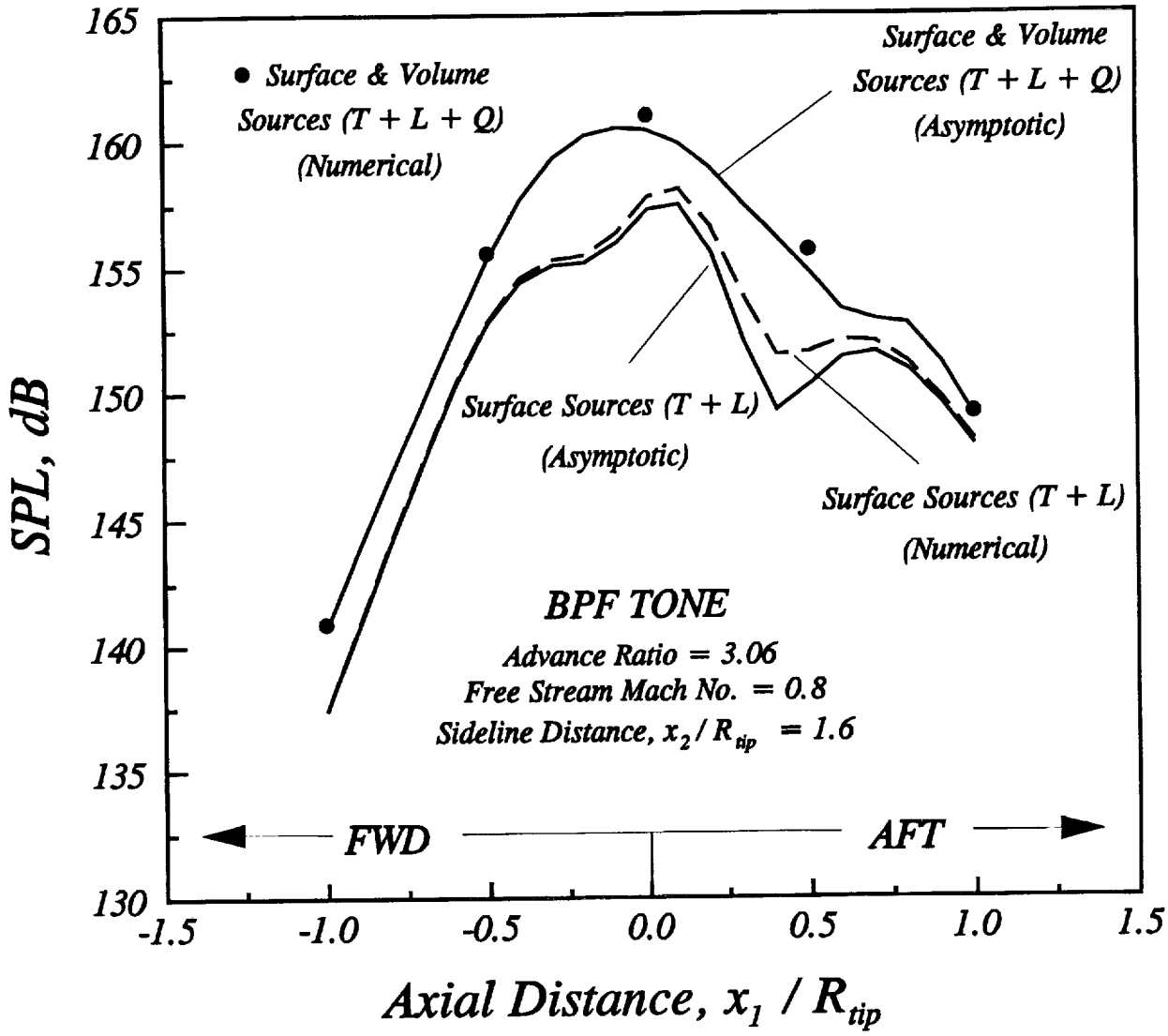

Fig. (4) Sideline Directivity of Thickness + Loading + Quadrupole and Thickness + Loading SPLs. Comparison of Asymptotic and Numerical Results.

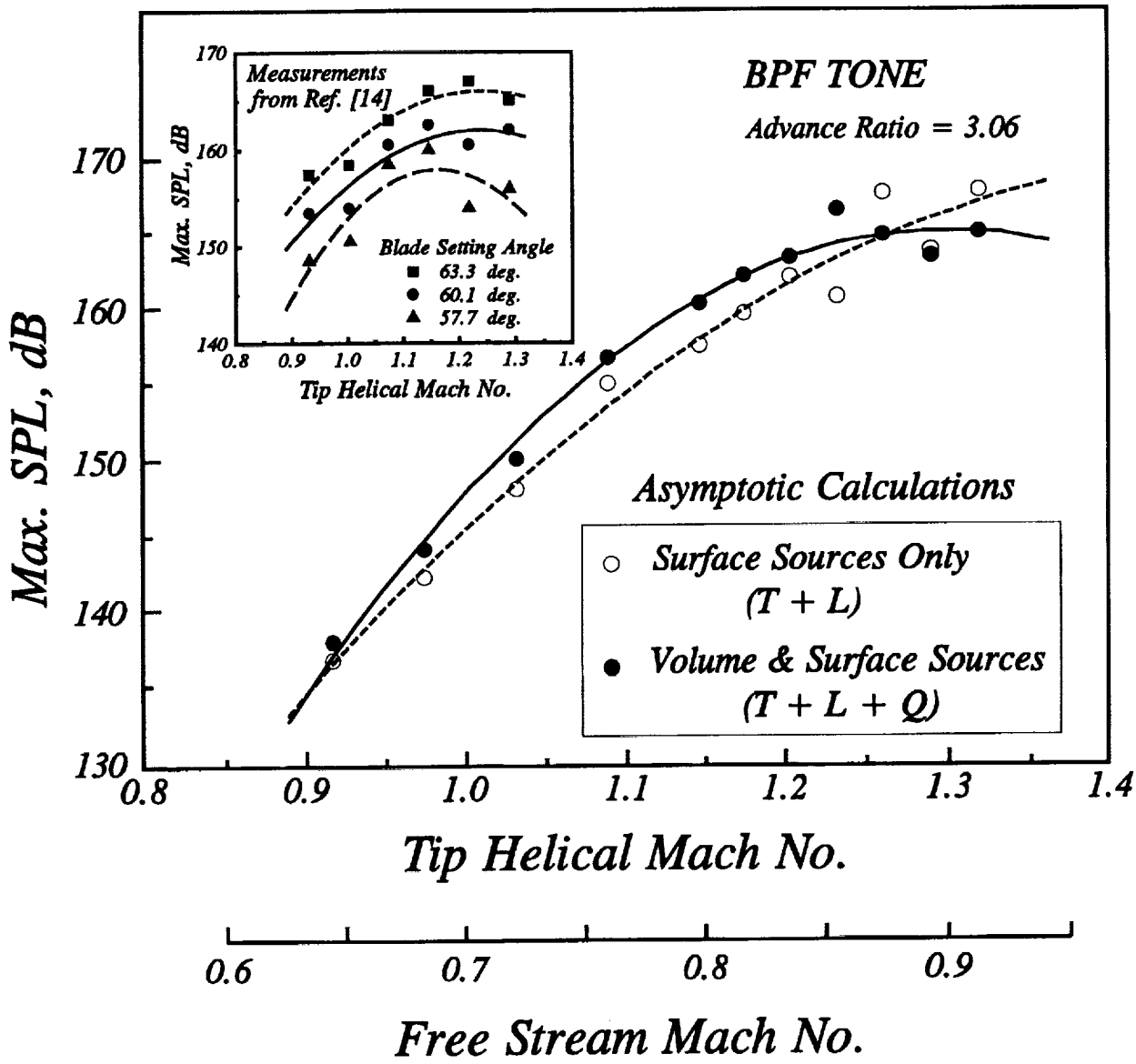

Fig. (5) Predicted Variations of Peak Thickness + Loading + Quadrupole and Thickness + Loading SPLs with Tip Helical Mach Number. Inset: Experimental Data.

REPORT DOCUMENTATION PAGE

Form Approved
OMB No. 0704-0188

1. AGENCY USE ONLY (Leave blank)	2. REPORT DATE	3. REPORT TYPE AND DATES COVERED
	May 1992	Final Contractor Report

4. TITLE AND SUBTITLE

An Asymptotic Theory of Supersonic Propeller Noise

5. FUNDING NUMBERS

WU-535-03-10
C-NAS3-25266

6. AUTHOR(S)

Edmane Envia

7. PERFORMING ORGANIZATION NAME(S) AND ADDRESS(ES)

Sverdrup Technology, Inc.
Lewis Research Center Group
2001 Aerospace Parkway
Brook Park, Ohio 44142

8. PERFORMING ORGANIZATION REPORT NUMBER

E-7723

9. SPONSORING/MONITORING AGENCY NAMES(S) AND ADDRESS(ES)

National Aeronautics and Space Administration
Lewis Research Center
Cleveland, Ohio 44135-3191

10. SPONSORING/MONITORING AGENCY REPORT NUMBER

NASA CR-191110

11. SUPPLEMENTARY NOTES

Prepared for the 14th Aeroacoustics Conference sponsored by the DGLR and AIAA, Aachen, Germany, May 11-14, 1992. Project Manager, J. Groeneweg, Propulsion Systems Division, NASA Lewis Research Center, (216) 433-6751.

12a. DISTRIBUTION/AVAILABILITY STATEMENT

Unclassified - Unlimited
Subject Category 71

12b. DISTRIBUTION CODE

13. ABSTRACT *(Maximum 200 words)*

A theory for predicting the noise field of supersonic propellers with realistic blade geometries is presented. The theory, which utilizes a large-blade-count approximation, provides an efficient formula for predicting the radiation of sound from all three sources of propeller noise. Comparisons with a full numerical integration indicate that the levels predicted by this formula are quite accurate. Calculations also show that, for high speed propellers, the noise radiated by the Lighthill quadrupole source is rather substantial when compared wth the noise radiated by the blade thickness and loading sources. Results from a preliminary application of the theory indicate that the peak noise level generated by a supersonic propeller initially increases with increasing tip helical Mach number, but it eventually reaches a plateau and does not increase further. The predicted trend shows qualitative agreement with the experimental observations.

14. SUBJECT TERMS

Supersonic propeller noise; Uniform asymptotic theory; Quadrupole radiation

15. NUMBER OF PAGES
20

16. PRICE CODE
A03

17. SECURITY CLASSIFICATION OF REPORT	18. SECURITY CLASSIFICATION OF THIS PAGE	19. SECURITY CLASSIFICATION OF ABSTRACT	20. LIMITATION OF ABSTRACT
Unclassified	Unclassified	Unclassified	